Title

E-cigarette aerosol impairs male mouse skeletal muscle force development and prevents recovery from injury

Journal

AJP Regulatory Integrative and Comparative Physiology, 323(6)

ISSN

0363-6119

Authors

Nogueira, Leonardo
Zemljic-Harpf, Alice E
Yusufi, Raihana
et al.

Publication Date

2022-12-01

DOI

10.1152/ajpregu.00314.2021

Peer reviewed

AMERICAN JOURNAL OF PHYSIOLOGY
REGULATORY, INTEGRATIVE AND COMPARATIVE PHYSIOLOGY

Am J Physiol Regul Integr Comp Physiol 323: R849–R860, 2022.
First published October 17, 2022; doi:10.1152/ajpregu.00314.2021

RESEARCH ARTICLE

Don't Deny Your Inner Environmental Physiologist: Investigating Physiology with Environmental Stimuli

E-cigarette aerosol impairs male mouse skeletal muscle force development and prevents recovery from injury

Leonardo Nogueira,[1,5] Alice E. Zemljic-Harpf,[2,3] Raihana Yusufi,[1] Maryam Ranjbar,[4] Christopher Susanto,[4] Kechun Tang,[3] Sushil K. Mahata,[1,3] Patricia A. Jennings,[4] and Ellen C. Breen[1]

[1]*Department of Medicine, University of California, San Diego, La Jolla, California;* [2]*Department of Anesthesiology, University of California, San Diego, La Jolla, California;* [3]*Veterans Affairs San Diego Healthcare System, San Diego, California;* [4]*Department of Chemistry and Biochemistry, University of California, San Diego, La Jolla, California; and* [5]*School of Exercise and Nutritional Sciences, College of Health and Human Services, San Diego State University, San Diego, California*

Abstract

To date, there has been a lag between the rise in E-cigarette use and an understanding of the long-term health effects. Inhalation of E-cigarette aerosol delivers high doses of nicotine, raises systemic cytokine levels, and compromises cardiopulmonary function. The consequences for muscle function have not been thoroughly investigated. The present study tests the hypothesis that exposure to nicotine-containing aerosol impairs locomotor muscle function, limits exercise tolerance, and interferes with muscle repair in male mice. Nicotine-containing aerosol reduced the maximal force produced by the extensor digitorum longus (EDL) by 30%–40% and, the speed achieved in treadmill running by 8%. Nicotine aerosol exposure also decreased adrenal and increased plasma epinephrine and norepinephrine levels, and these changes in catecholamines manifested as increased muscle and liver glycogen stores. In nicotine aerosol exposed mice, muscle regenerating from overuse injury only recovered force to 80% of noninjured levels. However, the structure of neuromuscular junctions (NMJs) was not affected by e-cigarette aerosols. Interestingly, the vehicle used to dissolve nicotine in these vaping devices, polyethylene glycol (PG) and vegetable glycerin (VG), decreased running speed by 11% and prevented full recovery from a lengthening contraction protocol (LCP) injury. In both types of aerosol exposures, cardiac left ventricular systolic function was preserved, but left ventricular myocardial relaxation was altered. These data suggest that E-cigarette use may have a negative impact on muscle force and regeneration due to compromised glucose metabolism and contractile function in male mice.

NEW & NOTEWORTHY In male mice, nicotine-containing E-cigarette aerosol compromises muscle contractile function, regeneration from injury, and whole body running speeds. The vehicle used to deliver nicotine, propylene glycol, and vegetable glycerin, also reduces running speed and impairs the restoration of muscle function in injured muscle. However, the predominant effects of nicotine in this inhaled aerosol are evident in altered catecholamine levels, increased glycogen content, decreased running capacity, and impaired recovery of force following an overuse injury.

exercise; lengthening contraction; neuromuscular; vaping

INTRODUCTION

The popularity of E-cigarette use in the past several years has been alarming (1, 2). This became evident in 2018 with a rapid rise in lung injury, referred to as E-cigarette and vaping product-associated lung injury (EVALI), which presented a mortality greater than 2% (3). Youth that use E-cigarettes or traditional tobacco cigarettes, particularly dual users, have been reported to abstain from moderate or vigorous physical activity (4). Whether pathological changes in striated muscle contribute to this exercise avoidance are not well understood. Furthermore, the long-term consequences of inhaling these high levels of nicotine in a heated aerosolized mixture of propylene glycol (PG), vegetable glycerin (VG) along with artificial flavoring and unknown contaminants has not been fully interrogated.

E-cigarette use is associated with several systemic effects that include inflammation, oxidative stress, and altered central nerve activity (5–17). Activation of these processes can impact cardiac function by inducing carotid artery and aortic stiffness and increasing sympathetic nerve activity. These cardiovascular changes can stimulate abnormal heart rate

Correspondence: E. C. Breen (ebreen@health.ucsd.edu).
Submitted 21 December 2021 / Revised 5 October 2022 / Accepted 6 October 2022

variability and sustained increases in blood pressure (17–24). Chen et al. (25) recently reported that mice exposed to E-cigarette aerosol containing 5 mg/mL of nicotine and artificial flavoring over a short-term period of 14 days demonstrated impaired exercise performance in tests of grip strength and swimming endurance that was accompanied by decreased liver and muscle glycogen content. Previous studies have demonstrated differential effects of acute versus chronic nicotine and adrenergic stimuli on glucose metabolism and glycogen storage (26, 27). Chronic nicotine itself has been reported to increase the release of catecholamines that can alter glucose uptake and glycogenolysis and contribute to muscle weakness (28–30). Chronic stimulation by nicotine also modifies skeletal muscle Na-K-ATPase activity through its interaction with neuronal-type acetylcholine receptors (nAChRs) located both on central motor neurons and peripheral myofibers (31, 32). Smoking traditional tobacco cigarettes, the most widely used nicotine delivery device, has been shown to lead to changes in peripheral muscle atrophy, oxidative to glycolytic fiber-type transition, capillary regression, and altered myofiber calcium handling, which contribute to reduced exercise performance (33–35). These changes in myofiber structure and function are thought to be preceded by degeneration of the neuromuscular junctions (NMJs) that innervate locomotor myofibers (36). However, the effect of E-cigarette components, with known changes in vascular networks, inflammatory cytokines, and reactive oxygen species, in addition to very high nicotine levels, on muscle function has not been fully elucidated.

In this study, we hypothesized that the high levels of nicotine, delivered through the inhalation of E-cigarette aerosol, would impair the degeneration-regeneration process of peripheral NMJs, decrease muscle force, and limit exercise tolerance. This was tested by measuring treadmill running exercise performance, cardiac function by echocardiogram, and isolated muscle contractile function in noninjured and regenerating muscles in male mice. Changes in adrenal gland and plasma catecholamines that could regulate glycogen stores in the liver and peripheral muscles were measured. The integrity of the peripheral neuromuscular transmission system was evaluated by morphometric analysis of the NMJs.

MATERIALS AND METHODS

Ethical Approval

This study was approved by the University of California, San Diego Animal Care and Use Committee (Protocol No. S01144) and complies with the American Physiological Society's Guiding Principles in the Care and Use of Vertebrate Animals in Research and Training. Male B6.Cg-Tg(Thy1-YFP)16Jrs/J mice (2–4 mo of age) from The Jackson Laboratory (Cat. No. 003709) were housed 3–4 per cage in a pathogen-free vivarium, maintained on a 12:12-h day-night cycle and provided standard chow (Harlan Tekland 8604, Madison, WI) and tap water ad libitum. Mice were randomly assigned to nonexposed (n = 22 mice), PG/VG (n = 15 mice), and PG/VG + Nicotine (n = 16 mice) groups. Mice were exercise tested before the exposure protocols. They were again exercise tested at the 3-mo time point before being subjected to a lengthening contraction protocol (LCP). After all functional assessments were completed at 4 mo, mice were euthanized by surgical removal of the heart while under anesthesia (ketamine:xylazine, 100:10 mg/kg ip). All experimenters were blinded to the exposure groups.

Exposure to E-Cigarette Aerosol

Mice were exposed using the In Expose System with a whole body chamber (total volume of 5 L divided into 16 compartments) from SCIREQ (Montreal, QC, Canada). Mice were exposed to E-liquid that was heated and aerosolized in a SUBTANK Plus 7.0 mL from Kanger Tech [Shenzhen, China (1.8 Ohm) and attached to a rechargeable lithium-ion battery (2.5–4.1 V)]. All components and dispensers were obtained from Xtreme Vaping. The E-cigarette aerosol was generated from liquid containing 6 mg/mL of nicotine (Sigma, No. N3876), which is commonly utilized by E-cigarettes users and is on the low end of the nicotine range (37), in 30% PG (Sigma Aldrich, No. 134368) and 70% VG (Sigma Aldrich, No. G7757). The ratio of PG/VG is often recommended for E-cigarette users of tank systems. In a separate, whole body chamber, additional mice were exposed to aerosol without nicotine (PG/VG). For some experiments, mice were placed in a third whole body chamber and exposed to room air (AIR). Nonexposed mice that remained in their cages were also used as a control group. Mice were exposed for 4 s out of every 20 s (12 s/min total) at a flow rate of ~3 L/min for 30 min, then allowed a fresh-air period of 30 min followed by a second 30-min vaping period. Mice were exposed 5 days each week for 4 mo. Previous studies from our group utilizing male mice revealed that tobacco cigarette smoke exposure impairs skeletal muscle contractile function starting at 2 mo of exposure and reaching a steady state at 4 mo of exposure (33, 34). Different e-liquid tanks and exposure chambers were used for each group to avoid cross contamination.

Treadmill Exercise Test

Two days before each exercise test, mice were familiarized on a treadmill (model CL-4, Omnitech, Columbus, OH) by running for 10 min at 10–15 cm/s on a 10° incline. Maximal speed was measured by running each mouse at 33 cm/s for 1 min and increasing the speed by 3–4 cm/s each minute until exhaustion. Mice were deemed exhausted at the point in which they could not remain on the treadmill and sat on the shock grid (≤0.3 mA) for 8 s. Mice were tested before the exposure protocol was initiated and 3 months later (before the LCP).

Lengthening Contraction Protocol

Mice were anesthetized with 2.5% isoflurane. The right leg was shaved. The mice were then placed in a supine position in a home-built LCP system and maintained under 1.0% to 1.5% isoflurane. The right knee was secured in place and the right foot was attached to a lever plate. Electrodes were placed on either side of the common peroneal nerve, which innervates the anterior crural muscles including the tibialis anterior (TA) and the extensor digitorum longus (EDL). Correct electrode placement was confirmed by a single train (300 ms trains, 2 V, 0.5 ms square-waved pulses, 100 Hz pulse frequency) with an S88X stimulator. For each mouse,

the optimal voltage was set by monitoring torque as the voltage applied was increased in 0.5-V increments with 2-min intervals between stimulations until the maximum torque was reached. The lengthening contractions were then run at the optimal voltage (V) and at 150 Hz pulse frequency. The muscle lengthening injury was produced by superimposing a muscle lengthening (plantar flexion) during the last 200 ms of the contraction period (2 s) for 5 min (150 contractions total) and repeated two more times with 5-min rest periods between each LCP bout (70).

Transthoracic Echocardiography

Echocardiography (ECG; M-mode, two-dimensional, tissue Doppler and, pulse-wave Doppler) was performed under isoflurane anesthesia (1%–1.5% at a flow rate of 1 L/min oxygen) using a small-animal, high-resolution Vevo 3100 imaging unit (MX550S 26–52 MHz transducer, FUJIFILM VisualSonics, Toronto, Canada). For the assessment of systolic function and tissue Doppler analysis, ECG-traced heart rates were maintained between 520 and 600 beats/min to avoid anesthesia-induced changes in cardiac function. To assess systolic cardiac function, left ventricular ejection fraction (%EF), fractional shortening (%FS), mean circumferential fiber shortening rate (VCF) (38), and wall thickness were measured, as previously described (39). We further performed tissue Doppler imaging to measure early diastolic mitral annular velocity (E'). This parameter evaluates left ventricular myocardial relaxation in the longitudinal direction (40). E is the early diastolic transmitral valve flow velocity measured by pulse-wave Doppler. The ratio of these values (E/E') estimates left ventricle filling pressure. Late diastolic mitral annular velocity (A) was also measured by pulse-wave Doppler. Thus, E/A is used to assess diastolic function by early (E) to late (A) diastolic transmitral valve blood flow velocities (40, 41). Pulse-wave Doppler measurements were collected at heart rates between 400 and 450 beats/min (to separate E and A waves). The sonographer was blinded to the experimental groups.

Determination of Catecholamines by Ultrapressure Liquid Chromatography

Adrenal and plasma catecholamines were determined with an ACQUITY UPLC H-Class System fitted with an Atlantis dC18 column (100 Å, 3 μm, 3 mm × 100 mm) and connected to an electrochemical detector (ECD model 2465, Waters Corp, Milford, MA) as described previously (42). Fresh-frozen adrenal glands were homogenized in 250 μL of cold phosphate-buffered saline (PBS) for 30 s, and an aliquot of the homogenate was used for protein concentration assay. Homogenate (200 μL) was acidified by carefully mixing with cold HCl (0.2 N) and centrifuged at 8,000 rpm/4°C for 15 min. 3,4-Dihydroxybenzylamine [DHBA (400 ng): internal standard], and 30 mg of activated alumina were added to the supernatant and titrated with Tris buffer to pH 8.6. Catecholamines were adsorbed onto activated alumina in a shaker for 30 min at room temperature. Alumina beads were washed twice with 500 μL of water by gentle swirling followed by centrifugation and removal of water. Adsorbed catecholamines were eluted with 200 μL of 0.1 N HCl and centrifuged at 12,000 rpm for 2 min. Supernatant was passed through a Corning Costar Spin-X centrifuge tube filters (Sigma Aldrich, Cat No. CLS8162). Filtered solution was used for catecholamine assay. The mobile phase (isocratic: 0.3 mL/min) consisted of phosphate-citrate buffer and acetonitrile at 95:5 (vol/vol). The ECD was set at 50 nA for determination of adrenal norepinephrine and epinephrine. For determination of plasma catecholamines, DHBA (2 ng) was added to 150 μL of plasma and adsorbed with ~15 mg of activated aluminum oxide for 10 min in a rotating shaker. After being washed with 1 mL of water, adsorbed catecholamines were eluted with 100 μL of 0.1 N HCl. The ECD was set at 500 pA for determination of plasma catecholamines. Data were analyzed using Empower software (Waters Corp., Milford, MA). Catecholamine levels were normalized with the recovery of the internal standard expressed as nM (plasma) or nmol/mg protein (adrenal gland).

Colorimetric Determination of Tissue Glycogen Content

Glycogen was extracted from liver (25–30 mg) and gastrocnemius muscle (100–120 mg) by boiling tissues with 30% KOH as described previously (43). Alkaline-extracted glycogen from tissues was cold-precipitated with 66% ethanol and washed with 70% ethanol. After being dried to remove traces of ethanol, the pellets were dissolved in double-distilled water and then subjected to colorimetric determination of glycogen using anthrone reagent (0.05% anthrone and 1% thiourea) in concentrated H_2SO_4. Bovine liver glycogen was used as a standard. The standard curve was prepared with 0, 15.62, 31.25, 62.5, 125, 250, 500, and 1,000 μg/mL of glycogen. Absorbance readings were collected with a Beckman Coulter DU730 spectrophotometer.

Ex Vivo Muscle Force

The EDL from both the LCP and contralateral, noninjured hindlimb were carefully dissected under a microscope and placed in ice-cold Tyrode solution (121 mM NaCl, 5 mM KCl, 1.8 mM $CaCl_2$, 0.5 mM $MgCl_2$, 0.4 mM NaH_2PO_4, 24 mM $NaHCO_3$, 5.5 mM glucose, 0.1 mM EGTA, containing 25 μM *d*-tubocurarine). Each muscle was mounted in an experimental chamber (800MS, Danish Myo Technology), and muscles were constantly perfused with Tyrode solution that was continuously bubbled with 95% O_2-5% CO_2 (final pH 7.4, 22°C). EDLs were electrically stimulated (S88X stimulator, Grass Technologies) using square-wave pulses (16 V; EDL: 250 ms train duration, 0.5 ms pulses). L_0 was determined with single twitches and muscles allowed to rest for 15 min. Contractile function was evaluated by stimulating the muscles at different pulse frequencies (1–150 Hz) with 100-s intervals. After the contractile protocol, muscles were blotted dry and weighed to determine the muscle cross-sectional area (CSA). Force development was normalized with respect to the muscle CSA (kPa) (44).

Muscle Mounts for NMJ Analysis

TAs were collected and initially placed in 2% paraformaldehyde followed by 30% sucrose overnight, respectively, for fixing. Fiber bundles were then separated from the deep region of the TA using a dissecting microscope. Fibers were subjected to blocking buffer containing 5% normal goat serum (NGS), 5% BSA, 2% Triton X-100 in phosphate-buffered

saline (PBS) overnight, and then incubated overnight again with Alexa594-conjugated α-bungarotoxin to identify acetylcholine receptors (AChR) (Thermo Fisher Scientific, 5 μg/mL concentration). Muscle bundles were washed with PBS three times for 10 min each and then mounted on slides with ProLong Gold Antifade Mountant (Cat No. P36930, Thermo Fisher Scientific). After curing, slides were sealed and stored in the dark at 4°C until imaged. Presynaptic motor neuron terminals are labeled with yellow fluorescent protein in B6.Cg-Tg (Thy1-YFP)16Jrs/J mice. Thy1-YFP and Alexa594-conjugated α-bungarotoxin signals were detected by confocal microscopy with a Leica SP8 confocal with lightening deconvolution system using a ×20 magnification and 488 nm and 594 nm lasers. NMJ image stacks that contained entire NMJs were collected. NMJ image stacks were collected with pre-established parameters [400 dpi, 60%–80% gain, speed 500 Hz–700 Hz, no offset, Z stack (100–200 μm range)] for all samples. Maximal intensity projections were obtained using LASX software before analysis with Fiji. NMJ morphology was characterized for en face endplates based on the following parameters: *1*) total endplate area, *2*) endplate perimeter, and *3*) pre- and postsynaptic apposition (% of apposition between the axon terminal and underlying AChRs). The number of NMJs analyzed per exposure group (~50 NMJs/mouse; $n = 6$) are the following: AIR group, 321; PG/VG group, 307, and E-CIG group, 318. Approximately, half of the NMJs analyzed were either from the noninjured TA or the TA injured with the LCP. Image analyses were performed by one observer who was blinded to the identity of the samples.

Statistical Analysis

All data are presented as the means ± standard deviation (SD). A P value less than 0.05 was considered significantly different. Analyses of NMJs were determined by comparing the mean NMJ parameters in each mouse ($n = 6$ mice) using two-way ANOVA followed by Bonferroni's post hoc testing. The main variables were LCP injury and exposure group. Force-frequency curves were analyzed using a two-way ANOVA with exposure group and frequency as the main variables and Bonferroni's post hoc tests. The running speeds were analyzed by two-way ANOVA with exposure group and exercise tests performed before and after exposure as the main variables followed by Bonferroni's post hoc testing. Catecholamines and glycogen levels were analyzed using one-way ANOVA and Tukey's post hoc tests. Cardiac parameters were analyzed using a one-way ANOVA and Dunnette's post hoc tests. Normality distribution test (D'Agostino & Person) showed that data were normally distributed ($\alpha = 0.05$). All the analyses were conducted using GraphPad Prism version 9.00 (San Diego, CA).

RESULTS

Effect of E-Cigarette Aerosol on NMJ Innervation

Innervation of NMJs in the TA was evaluated 28 days after the LCP by measuring end-plate area and perimeter and the percentage of pre- and postsynaptic apposition. Figure 1*A* shows representative presynaptic motor neurons labeled with YFP and postsynaptic NMJs detected with Alexa594-conjugated α-bungarotoxin in LCP recovered TA fiber bundles (Supplemental Fig. S1; see https://doi.org/10.6084/m9.figshare.17138657.v1). Morphometric analysis of endplate area did not reveal an overall difference between groups (two-way ANOVA: exposure group, $P = 0.64$, injury, $P = 0.26$, interaction, $P = 0.18$, Fig. 1*B*). No differences were observed in NMJ perimeter between the groups (two-way ANOVA: exposure group, $P = 0.99$, injury, $P = 0.94$, interaction, $P = 0.37$, Fig. 1*C*). Analysis of the percent pre- and postapposition did not reveal differences between exposure groups and LCP injury (two-way ANOVA, exposure group, $P = 0.075$, injury, $P = 0.61$, interaction, $P = 0.27$, Fig. 1*D*). The size distribution of NMJs in noninjured muscles revealed a difference between the AIR and the PG/VG and PG/VG + Nicotine exposure groups (two-way ANOVA: NMJ area, $P < 0.0001$, group, $P = 1.00$ interaction, $P < 0.0001$, Fig. 1*E*). The PG/VG and PG/VG + Nicotine groups showed an increased number of NMJs in the range of 200–250 μm^2 compared with the AIR group ($P < 0.001$ for both AIR versus PG/VG and AIR versus PG/VG + Nicotine, Bonferroni posttest, Fig. 1*E*). The distribution of NMJ size was not different between exposure groups in the LCP-injured muscles (two-way ANOVA: NMJ area, $P < 0.0001$, group, $P = 1.00$ interaction, $P = 0.1510$, Fig. 1*F*).

Decreased Ex Vivo EDL Force Production in Mice Exposed to E-Cigarette Aerosol

PG/VG and PG/VG + Nicotine groups did not show a decrease in heart, TA, soleus, plantaris, or gastrocnemius mass (data not shown). Male mice in the PG/VG and PG/VG + Nicotine groups weighed less than nonexposed mice (Supplemental Fig. S2; see https://doi.org/10.6084/m9.figshare.17138810.v1). Isolated EDL, previously subjected (i.e., 28 days before) to in vivo lengthening contractions, and the contralateral, noninjured, EDL were tested for changes in contractile function. In noninjured EDL from PG/VG + Nicotine male mice, contractions evoked by submaximal and maximal frequencies of stimulation were weaker than in the EDL from nonexposed and air-exposed male mice (two-way ANOVA, exposure group, $P < 0.0001$, pulse-freq, $P < 0.0001$, interaction, $P = 0.52$, Fig. 2*A*). The maximum tetanic force produced by EDL from PG/VG + Nicotine male mice was 30% lower than EDL from nonexposed male mice (373 ± 48 kPa vs. 440 ± 52 kPa vs. 351 ± 101 kPa vs. 260 ± 103 kPa, for nonexposed vs. Air vs. PG/VG vs. PG/VG + Nicotine, respectively, $P < 0.0001$, Bonferroni posttest, Fig. 2*A*). In EDL recovered from LCP injury, the force developed over a range of submaximal and maximal frequencies of stimulation were reduced in both PG/VG and PG/VG + Nicotine groups compared with nonexposed and AIR groups (two-way ANOVA, exposure group, $P < 0.0001$, pulse-freq, $P < 0.0001$, interaction, $P = 0.96$, Fig. 2*B*). Maximum force produced by EDL from the PG/VG and PG/VG + Nicotine exposed mice were both 22% lower than the maximal force of EDL from the nonexposed group (390 ± 58 kPa vs. 387 ± 125 kPa vs. 302 ± 42 kPa vs. 299 ± 70 kPa, for nonexposed vs. AIR vs. PG/VG vs. PV/VG + Nicotine, respectively, $P < 0.05$, $P < 0.01$, Bonferroni posttest, Fig. 2*B*). EDL mass, length, and cross-sectional area from both LCP and noninjured anterior crural muscles were not different between the groups (Supplemental Fig. S3; see https://doi.org/10.6084/m9.figshare.17138837.v1).

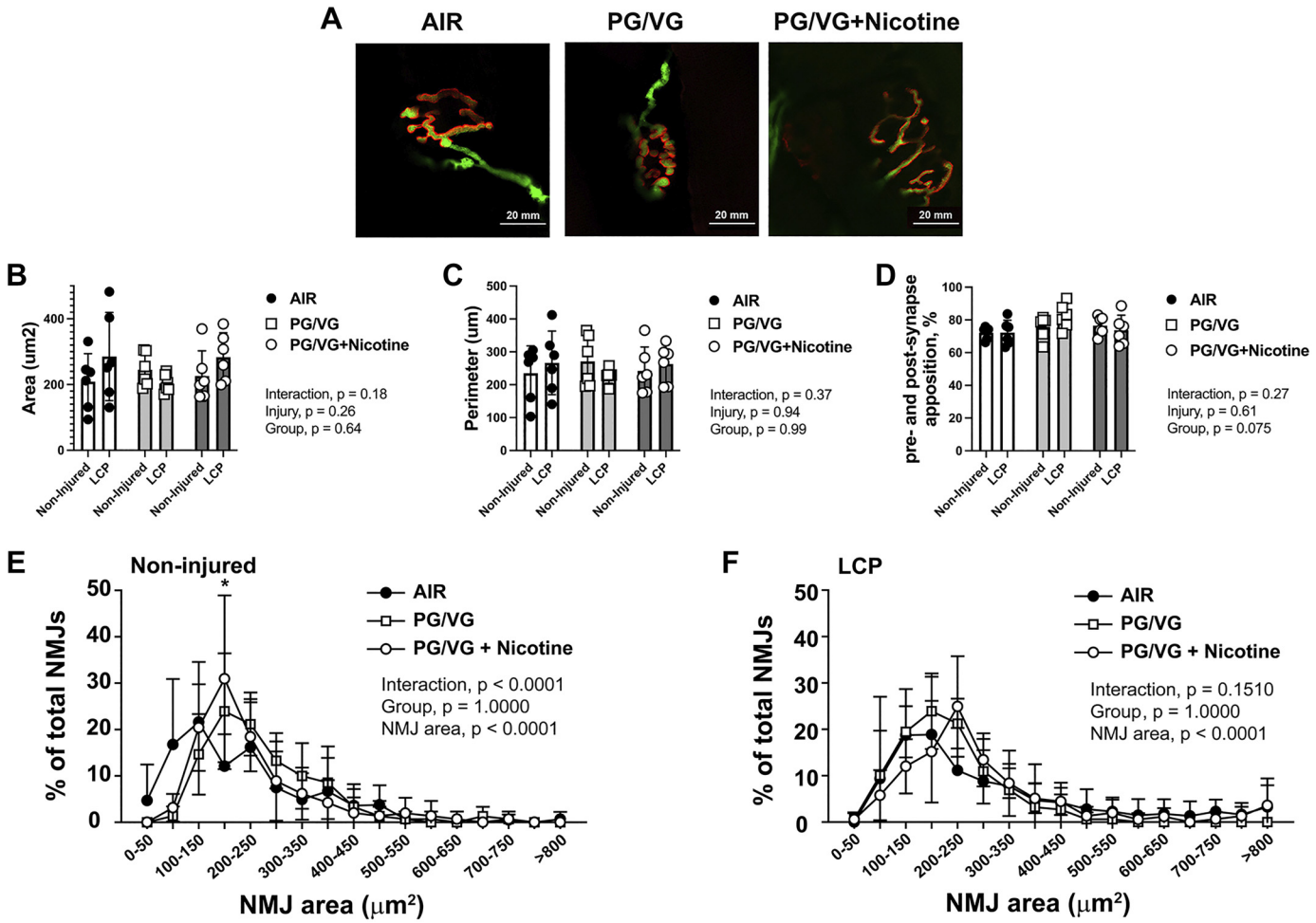

Figure 1. Neuromuscular junction (NMJ) morphology from noninjured and injured tibialis anterior muscles in mice exposed to E-cigarette aerosol components. *A*: representative NMJ images collected by confocal microscopy of each exposure group. Red—Alexa-594-α-bungarotoxin; Green—YFP labeled motor neurons. Scale bar = 20 μm. *B*: NMJ area. Two-way ANOVA, exposure group, $P = 0.64$; lengthening contraction protocol (LCP) injury, $P = 0.26$; interaction, $P = 0.18$. *C*: NMJ perimeter. Two-way ANOVA, exposure group, $P = 0.99$; LCP injury, $P = 0.94$; interaction, $P = 0.37$. *D*: pre- and postsynaptic apposition (%). Two-way ANOVA, exposure group, $P = 0.075$; LCP injury, $P = 0.61$; interaction, $P = 0.27$. *E* and *F*: percentage of total NMJs distributed by NMJ area from noninjured (*E*) and LCP injured (*F*) muscles. Two-way ANOVA, exposure group, $P = 1.000$; NMJ area, $P < 0.0001$; interaction, $P < 0.0001$ (*E*) and $P = 0.151$ (*F*). *$P < 0.001$, Bonferroni post hoc tests indicate a significant difference between the percentage of total NMJs in the polyethylene glycol (PG)/vegetable glycerin (VG) and PG/VG + Nicotine groups compared with room air (AIR) group in noninjured muscles (*E*). Images were collected from 6 mice in each group.

Exposure to E-Cigarette Aerosol Decreases Exercise Performance

Male mice in each group were exercise tested for the maximal speed that could be achieved in treadmill running tests before and after daily exposures over a 3-mo period. After the first 3 mo of the exposure period, statistical difference was detected in the two-way ANOVA for the time of exposure and the interaction between exposure group and time (Fig. 2*C*, exposure group, $P = 0.08$, time, $P < 0.0001$, interaction, $P < 0.03$). Comparison between pre- and postexposure periods (Bonferroni posttests) revealed an 11% decrease in PG/VG maximal speed ($P = 0.0005$) and an 8% decrease in PG/VG + Nicotine maximal speed ($P = 0.0003$), which was not detected in nonexposed maximal speed ($P > 0.05$). Soleus capillary density, capillary-to-fiber ratio, mean fiber area and fiber types were not different between groups (Supplemental Fig. S4; see https://doi.org/10.6084/m9.figshare.17138909.v3 and Supplemental Fig. S5; see https://doi.org/10.6084/m9.figshare.17138915.v1).

Adrenal and Plasma Catecholamines Levels in Response to E-Cigarette Aerosol Exposure

Acute or chronic exposure to nicotine induces catecholamine secretion from the adrenal gland as well as from chromaffin and PC12 cells (27, 45–47). Consistent with the existing literature, we found lower norepinephrine (NE) and epinephrine (Epi) levels in the adrenal glands isolated from male mice exposed to PG/VG + Nicotine than the PG/VG and AIR groups (Fig. 3, *A* and *B*, one-way ANOVA, NE $P = 0.0098$, Epi, $P = 0.0095$). Also, plasma catecholamines were different between groups (Fig. 3, *C* and *D*, one-way ANOVA, NE $P = 0.042$, Epi $P = 0.012$). There was a trend ($P = 0.06$) and significant ($P = 0.016$) increase in plasma norepinephrine and epinephrine, respectively, in PG/VG + Nicotine above

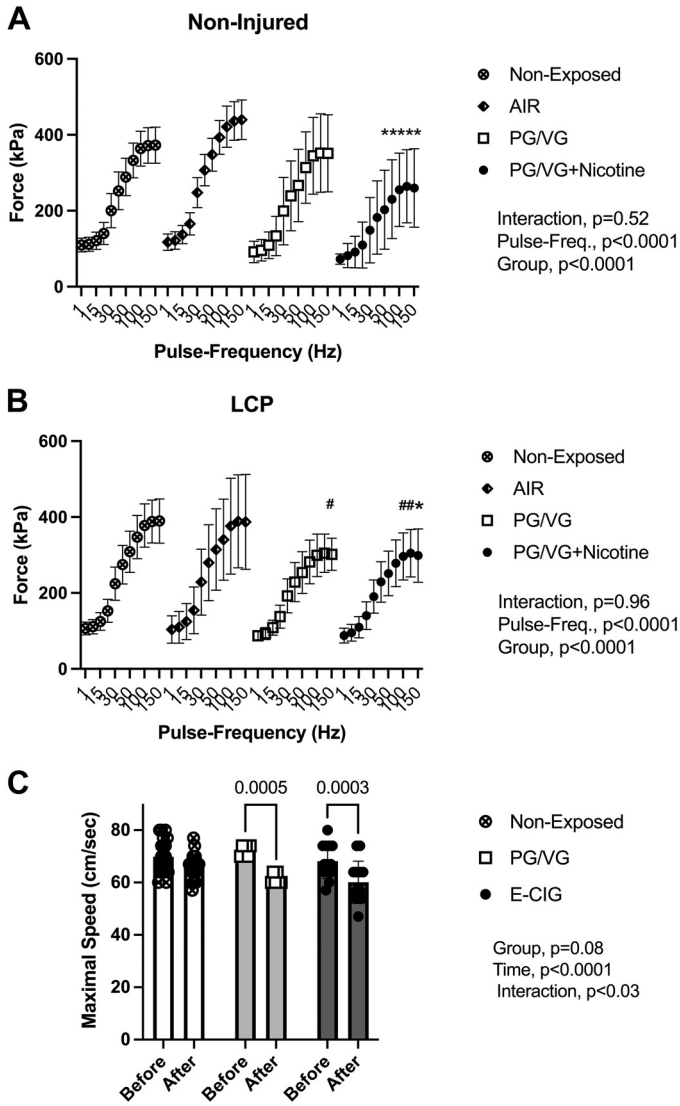

Figure 2. Integrated exercise performance and isolated extensor digitorum longus (EDL) function in mice exposed to vaping substances. Force-frequency relationship in noninjured (*A*) and lengthening contraction protocol (LCP)-injured skeletal muscle (*B*). Graphs of force (kPa) as a function of the stimulated pulse frequency are graphed for each exposure group for EDL dissected 28 days after the lengthening contraction protocol (LCP) and the contralateral, noninjured EDL. *$P <$ 0.01 Bonferroni post hoc tests indicate a significant difference in force between the polyethylene glycol (PG)/vegetable glycerin (VG) + Nicotine group and both the nonexposed and room air (AIR) group at the same pulse frequency. #$P < 0.05$ Bonferroni post hoc tests indicate a significant difference between force generated in the PG/VG + Nicotine group and the nonexposed groups at a given pulse frequency. Data are represented as the means ± SD, n = 11 nonexposed, n = 5 AIR, n = 4 PG/VG, n = 7 PG/VG + Nicotine. *C*: maximal running speed of E-cigarette exposed mice. Mice that were not exposed (nonexposed), exposed to vehicle oils without nicotine (PG/VG), or with nicotine (PG/VG + Nicotine) were exercise tested before and after a 3-mo period of daily exposures (Time). Two-way ANOVA indicates differences between before and after exposure (time) (group, $P = 0.08$, time, $P < 0.0001$, interaction, $P < 0.03$). In *C*, comparisons and *P* values obtained from Bonferroni post hoc tests are shown above bars and indicate a significant difference between the maximal running speed of mice in the PG/VG ($P = 0.0005$) and PG/VG + Nicotine ($P = 0.0003$) groups but not in the nonexposed group. Data are represented as the means ± SD. n = 22 nonexposed mice, n = 6 PG/VG mice, and n = 13 PG/VG + Nicotine mice.

AIR group values (Tukey posttests, Fig. 3, *C* and *D*). Exposure to PG/VG + Nicotine increased glycogen content in both liver and muscle (Fig. 3, *E* and *F*, one-way ANOVA, liver $P <$ 0.0001, muscle, $P = 0.004$).

Cardiac Contractility and Relaxation

After 4 mo of the daily exposure periods (1 mo after the exercise test), cardiac dimensions and functional parameters were measured by echocardiograph in anesthetized male mice (Fig. 4, Supplemental Table S1; see https://doi.org/10.6084/m9.figshare.17138921.v2). Left ventricular systolic function was preserved and, no change was observed in the percent ejection fraction (one-way ANOVA, $P = 0.97$) or fractional shortening (one-way ANOVA, $P = 0.96$) between groups (Fig. 4, *A* and *D*, Supplemental Table S1). To assess diastolic function, mitral inflow velocities (color doppler inflow signal) and the motion of the mitral annulus (pulse-wave tissue doppler) were measured. Early (*E*) and late (*A*) filling, also presented as *E/A* ratio, was unchanged in all three groups (one-way ANOVA, $P < 0.92$, Supplemental Table S1). Early (E') and late (A') mitral annular velocities were detected by transmural tissue Doppler. E', a parameter indicative of left ventricular myocardial relaxation during diastole, showed a reduction in velocity in both the PG/VG ($P =$ 0.029) and PG/VG + Nicotine groups ($P = 0.006$) when compared with nonexposed male mice (one-way ANOVA, $P =$ 0.007, Dunnett's posttests, Fig. 4*E*). A' remained unchanged (one-way ANOVA, $P = 0.12$, Supplemental Table S1). The ratio of early to late (E'/A') velocities between the groups was not different (one-way ANOVA, $P = 0.11$). E/E' ratios, a noninvasive measure of left ventricular filling pressure, assessed by the ratio of mitral peak velocity of early filling (*E*) to diastolic mitral annular velocity (E'), showed a statistical trend between groups (one-way ANOVA, $P = 0.07$; Fig. 4*F*). However, the left ventricular posterior wall dimension was reduced in the PG/VG group compared with the nonexposed and PG/VG + Nicotine groups (one-way ANOVA, $P < 0.005$, Supplemental Table S1). Individual echo parameters are presented in Supplemental Table S1.

DISCUSSION

The main findings of this study are as follows: *1*) male mice chronically exposed to nicotine containing E-cigarette aerosol demonstrated a decrement in exercise performance and incomplete restoration of locomotor muscle force following an overuse injury and *2*) chronic nicotine exposure leads to an increase in muscle and liver glycogen stores even in the presence of elevated plasma catecholamines. In addition, minor changes were observed in cardiac relaxation, but systolic function remained unchanged. No differences in NMJ morphometric parameters were detected that would suggest impaired NMJ function (i.e., pre-/postapposition or large fragmented NMJs). Minor changes in the size distribution of NMJs were observed in the E-cigarette aerosol exposure groups. All these factors could potentially contribute to prolonged muscle weakness particularly following exercise-induced muscle injury. Nicotine had a predominant negative effect on muscle contractility in both noninjured and regenerating muscle, but the vehicle used to deliver this substance, propylene glycol (PG) and

vegetable glycerin (VG) also prevented fully recovery of force after an overuse injury. Interestingly, both the high levels of nicotine and PG/VG alone without nicotine impaired exercise tolerance to the same extent. Together, these data suggest that the use of E-cigarettes could result in locomotor muscle dysfunction and altered energy metabolism and, these changes may contribute to users, particularly young adults, avoiding strenuous activity.

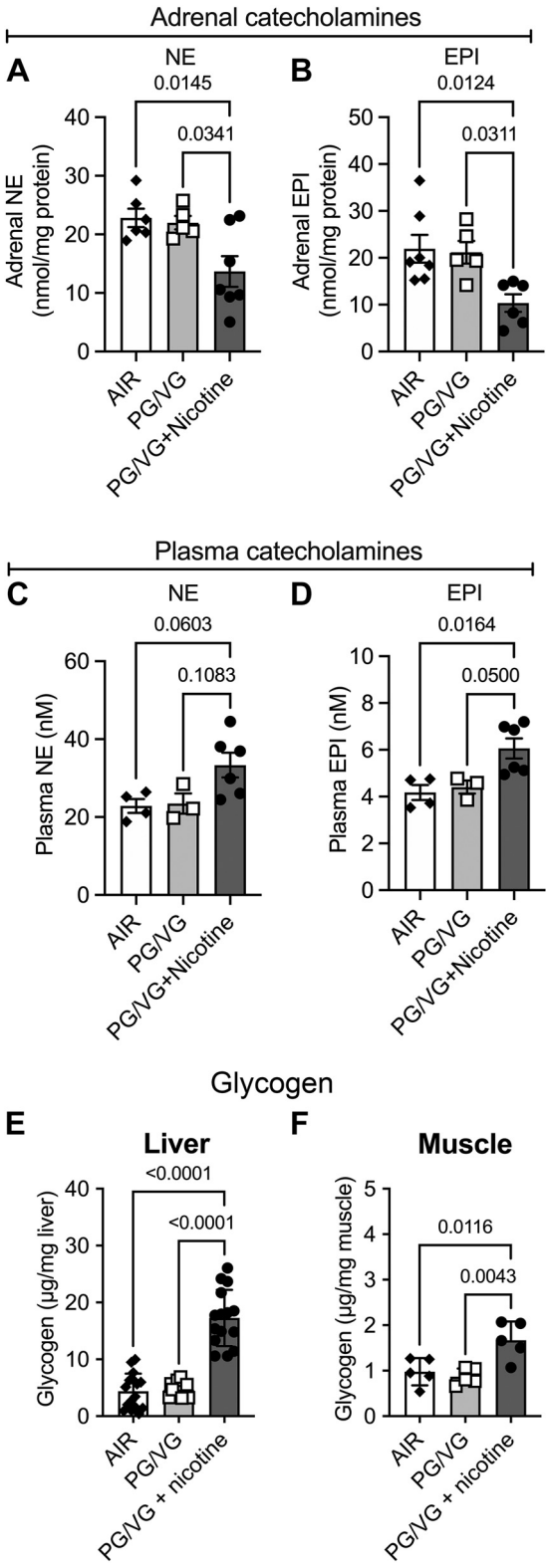

Decreased Exercise Performance and Impaired Skeletal Muscle Function with Chronic E-Cigarette Aerosol Exposure

Exercise capacity depends on a complex interaction between cardiac and vascular function, oxygen delivery, peripheral muscle activation and contractile function, and energy substrate utilization. In the present study, exercise performance was impaired in both the PG/VG and PG/VG + Nicotine groups. Even in the absence of a prior LCP injury, hindlimb muscles from PG/VG + Nicotine exposed male mice produced less force than muscle collected from the other exposure groups. The changes in muscle force were not related to EDL myofiber cross-sectional area. Thus, these data suggest that nicotine present in E-cigarette aerosol ultimately leads to a loss of muscle strength independently, or before, changes in muscle atrophy. Although the mechanism has not been fully elucidated, several studies have shown that chronic nicotine treatment may result in a net decrease in the activity of Na-K-ATPase, and subsequent membrane depolarization (32). The consequences of this steady membrane depolarization by chronic nicotine may result in impaired excitability and less activation of the contractile sites that ultimately inhibits excitation-contraction coupling during contraction. Remarkably, muscle and liver from PG/VG + Nicotine male mice showed much higher levels of glycogen (discussed in detail in *Role of Catecholamines in the Response to Chronic Nicotine E-Cigarette Exposure*). An overcompensation in glycogen storage could manifest some of the symptoms observed in glycogen storage diseases, such as McArdle's disease, in which excess glycogen stores found in skeletal muscle are associated with muscle degeneration and exercise intolerance (48). Conversely, in muscles previously injured by LCP and regenerated for 28 days, which is a sufficient recovery time for muscle to normally fully regenerate (49), EDL muscle force remained below noninjured levels in both exposure groups (PG/VG and PG/VG + Nicotine). A similar observation was detected in acute running tests. These data suggest that components present in heated aerosols have additional effects on muscle function and exercise capacity.

Role of Catecholamines in the Response to Chronic Nicotine E-Cigarette Exposure

Skeletal muscle displays increased force upon acute adrenergic stimulation (i.e., fight or flight response) (50, 51). It has been shown that phosphorylation of a single serine

Figure 3. Catecholamine (*A–D*) and glycogen (*E* and *F*) levels. Catecholamines were measured in the adrenal glands (*A* and *B*) and plasma (*C* and *D*). *A* and *B*: adrenal: norepinephrine:AIR, $n = 6$, polyethylene glycol (PG)/vegetable glycerin (VG), $n = 5$, PG/VG + Nicotine, $n = 7$. One-way ANOVA, $P = 0.0098$. epinephrine, AIR, $n = 7$, PG/VG, $n = 5$, PG/VG + Nicotine, $n = 6$. One-way ANOVA, $P = 0.0095$. *C* and *D*: plasma: norepinephrine (one-way ANOVA, $P = 0.042$) and epinephrine (one-way ANOVA, $P = 0.012$): AIR, $n = 4$, PG/VG, $n = 3$, PG/VG + Nicotine, $n = 6$. *E* and *F*: glycogen levels were measured in the liver (male and female mice), AIR, $n = 13$, PG/VG, $n = 15$, PG/VG + Nicotine, $n = 16$, one-way ANOVA, $P < 0.0001$ and gastrocnemius (Muscle) AIR, $n = 5$, PG/VG, $n = 5$, PG/VG + Nicotine, $n = 5$, one-way ANOVA, $P = 0.004$. For each panel, P values obtained after Tukey's post hoc tests from comparisons between exposure groups are shown above bars.

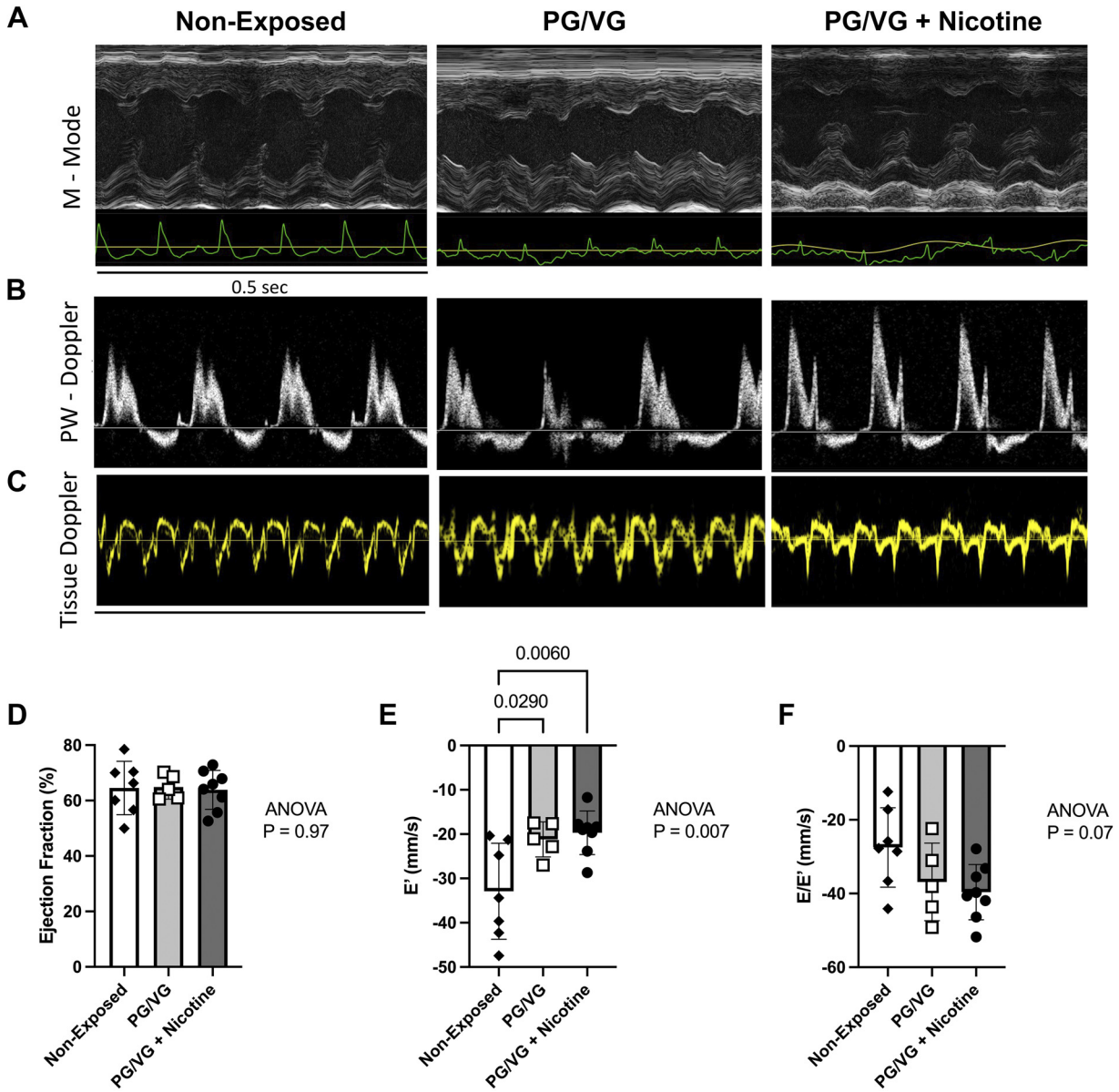

Figure 4. Echocardiogram and pulse-wave tissue Doppler measurements. *A*: M-Mode; *B*: PW-Doppler; *C*: tissue Doppler; *D*: ejection fraction (%); *E*: early diastolic ventricular mitral annular velocities (*E*′); *F*: noninvasive measure of left ventricular filling pressure (*E*/*E*′). Nonexposed (n = 7), polyethylene glycol (PG)/vegetable glycerin (VG) (n = 5), PG/VG + Nicotine (n = 8). One-way ANOVA and Dunnett's multiple-comparison posttest. Statistical differences between exposure groups, and the respective *P* values, obtained after Dunnett's posttests are indicated above graphs in (*E*).

residue (S2844) in the sarcoplasmic reticulum Ca^{2+} release channel/ryanodine receptor type 1 by protein kinase A is critical for acute stress-induced increase in contractile force (inotropy) (52). Consistent with existing literature, we report here that chronic elevation of plasma catecholamines result in muscle weakness (53, 54). In the present study, chronic exposure to nicotine containing E-cigarette aerosol caused a decrease of catecholamines, both epinephrine and norepinephrine, in the adrenal gland and a concomitant increase in circulating plasma catecholamines. We can speculate that chronic nicotine exposure present in E-cigarette aerosol alters the whole body catecholamine homeostasis either by increasing norepinephrine and epinephrine release into the plasma from the adrenal glands (27) or by decreasing catecholamine clearance due to a lower muscle and liver catecholamine action (55). Catecholamines act in myofibers and hepatocytes mainly through the β_2-adrenergic receptors to regulate carbohydrate metabolism (56–58). Among catecholamines, epinephrine is the most potent β_2-agonists (59) and, under physiological conditions, catecholamines enhance the rate of glycolysis (resulting in increased ATP resynthesis) in liver and muscle, and hepatic glucose production and output, from glycogenolysis and gluconeogenesis (57), as well as, inhibit insulin-mediated glycogenesis (60–62). In the present study, increased plasma epinephrine in response to E-cigarette aerosol is expected to do the aforementioned functions. These observations differ from the study of Chen et al. (25) in which a shorter E-cigarette aerosol exposure time (14 days) revealed both decreased muscle glycogen content and poor performance in grip-strength and swimming tests. Interestingly,

Chen et al. (25) used a vanilla-flavored E-liquid to expose mice to E-cigarette aerosols. The present investigation used unflavored E-liquid. This difference in E-liquid composition can produce changes in the outcomes between the two studies since it has been proposed that some flavors can alter cellular function and inflammatory signaling in mice exposed to E-liquid aerosols (63). However, it is also becoming increasingly evident that chronic exposure to nicotine or nicotine-receptor agonists increase peripheral insulin sensitivity in both rats and mice (27, 46, 64, 65). A recent study of diet-induced obese wild-type mice treated with the α3β4 nicotinic acetylcholine receptor agonist, 1,1-dimethyl-4-phenylpiperazinium iodide (DMPP), revealed improved glucose tolerance by stimulating nonoxidative glucose disposal into heart and gastrocnemius and quadriceps muscles (46). In support of this notion, the authors reported an increased incorporation of glucose into glycogen resulting in increased muscle glycogen content (46). Therefore, it is conceivable that the accumulation of muscle and liver glycogen in E-cigarette-exposed male mice in our study is due to the diversion of glucose from the glycolytic pathway to the glycogenic pathway. One of the major functions of insulin is to induce glycogenesis. We found increased glycogen content in liver and gastrocnemius muscle in E-cigarette aerosol exposed male mice. This finding is consistent with nicotine or nicotinic agonist-induced increase in insulin sensitivity (27, 46, 64, 65). In addition, high catecholamine levels have been known for many years to result in muscle weakness (53, 54). This may be due to their action on the motor neurons but also altered release of acetylcholine, changes in end-plate potential, and membrane depolarization at the NMJ-myofiber interface (66). Catecholamines can also regulate vessel reactivity and blood flow and have several differential effects on cardiac and skeletal muscle including apoptosis, proteolysis, and fibrosis. Thus, there are many systems that could be altered by chronic, sustained levels of epinephrine and norepinephrine that will require further investigation of chronic nicotine delivered through vaping devices.

Contribution of the Altered Cardiac Function

Previous studies in preclinical mouse models of E-cigarette exposure have provided evidence of possible cardiac dysfunction (20). Data from our group showed that CD-1 mice exposed to PG/VG with a high amount of nicotine (24 mg/mL) exposed over 6 mo developed cardiac fibrosis (22). The study reported by Olfert et al (24) demonstrated that C57Bl/6J mice exposed to E-cigarette aerosol containing 18 mg/mL over an 8-mo period led to aortic and carotid artery stiffness and impaired vascular reactivity, which is a risk factor for compromised cardiac function. Echocardiogram data from both the present study and that of Olfert et al (24) did not reveal changes in the cardiac output (percent ejection fraction) or fractional shortening. However, diastolic function was not measured in the earlier study by Olfert et al (24). In the present study, diastolic function, assessed by mitral inflow velocities using the Doppler *E*/*A* index (early to late diastolic transmitral flow), was unchanged. However, the early diastolic ventricular mitral annular velocity (E′), a marker for left ventricular relaxation, was reduced in both the PG/VG and PG/VG + Nicotine groups. In addition, there was a trend for left ventricle filling pressure estimated by the *E*/*E*′ index (the ratio of early mitral inflow velocity) to decrease. These data suggest increased left ventricular stiffness. In addition, there was some apparent thinning of the left ventricular posterior wall in diastole (LVPWd) in male mice exposed to PG/VG without nicotine. Reduced exercise tolerance is one clinical hallmark in patients presenting diastolic heart failure (also known as heart failure with preserved ejection fraction) because diastolic myocardial stiffness prevents the increase in left ventricular filling that is physiologically needed to increase the stroke volume during exercise (67). Further studies will be needed to determine if increasing the stress on the heart with a β-adrenergic stimulus, i.e., dobutamine, which more closely reflects exercise, will reveal greater impairments in cardiac function in E-cigarette-exposed male mice.

A Major Effect of Chronic E-Cigarette Aerosol on NMJ Morphology Was Not Present

In the present study, we used the LCP protocol to model the regeneration of NMJs after disruption from myofibers (68). Twenty-eight days after recovery from this type of overuse injury, male mice exposed to room air fully recovered muscle force and reinnervated the NMJs. In contrast, exposure to either aerosol, PG/VG or PG/VG + Nicotine, revealed a decrement in ex vivo muscle force production that was not accompanied by major changes in NMJ morphology. Minor change in the distribution of NMJ size was present particularly between the 200- and 250-μm^2 range. Although overt changes in NMJ structure and integrity were not detected, this finding does not preclude changes in the mechanism of NMJ transmission at the peripheral muscle. Previous studies have demonstrated that long-term nicotine inhibits NMJ transmission by producing steady depolarization of the membrane through isoform-specific inhibition and stimulation of the Na-K-ATPase α1 and α2, respectively, which interact with nAChR as part of an electrogenic complex (31). This steady decrease in depolarization has been proposed to limit the safety zone and contributes to a decrease in the endplate potential when the membrane is repeatedly depolarized during exercise or electronically stimulated to repetitively contract (32, 69). The NMJ morphometric data collected with nicotine E-cigarette vaping differs from the reported NMJ-myofiber denervation detected in patients with chronic obstructive pulmonary disease (COPD) and mice exposed to tobacco cigarette smoke (35, 36). Further studies will be required to explore potential nicotine-dependent mechanisms that may regulate NMJ functional transmission in response to E-cigarette aerosol.

Perspectives and Significance

Overall, data presented in this study suggest that the nicotine present in heated and aerosolized PG/VG has a major effect in stimulating the release of catecholamines, promoting the storage of glycogen in the liver and muscle, and impairing muscle force in male mice. Subjecting the muscle to an overuse type of injury (i.e., eccentric contractions) in male mice exposed to a nicotine-containing E-cigarette aerosol revealed an inability to fully restore muscle force. However, signals released by the vehicle alone (12, 20, 22)

can also limit exercise tolerance and prevent the recovery of muscle function following contraction-induced overuse injury. These data suggest that PG/VG and nicotine induce distinct changes in skeletal muscle, catecholamine levels, and glycogen storage, and these changes have the potential to inhibit contraction-induced force development.

Limitations

The present study only includes male mice. The potential sex difference in the response to E-cigarette aerosols will require further study. Furthermore, all exposures were performed in whole body exposure chambers and therefore, oral ingestion may contribute to the delivery of E-cigarette aerosols. Although the results from the present study clearly show that skeletal muscle functional and metabolic changes occur in male mice exposed to PG/VG with nicotine, E-cigarette aerosol users rarely use unflavored products, and therefore, the consequences of prolonged exposure to flavored E-cigarette aerosols will require further study.

SUPPLEMENTAL DATA

Supplemental Fig. S1: https://doi.org/10.6084/m9.figshare.17138657.v1.
Supplemental Fig. S2: https://doi.org/10.6084/m9.figshare.17138810.v1.
Supplemental Fig. S3: https://doi.org/10.6084/m9.figshare.17138837.v1.
Supplemental Fig. S4: https://doi.org/10.6084/m9.figshare.17138909.v3.
Supplemental Fig. S5: https://doi.org/10.6084/m9.figshare.17138915.v1.
Supplemental Table S1: https://doi.org/10.6084/m9.figshare.17138921.

ACKNOWLEDGMENTS

We thank Jennifer Santini and Marcella Erb for support and guidance in collecting the NMJ images by confocal microscopy. We also thank Dr. Richard Lovering for guidance in assembling and testing the LCP system based on his publication (70). Jenny Chiem, Makena Isley, Sami Marambashi, and Steven Vitorino exposed mice to E-cigarette components and assisted with sample collection. Anastasia Lucas exercise tested the mice, and Natalie K. Gilmore assisted in the muscle force measurements.

GRANTS

This research was supported by the Tobacco-Related Disease Research Program High Impact Pilot Award 26IP-0033S (to E. C. Breen), Tobacco-Related Disease Research Program New Investigator Award T29KT0397 (to L. Nogueira), and the U.S. Department of Veterans Affairs I01 BX003934 (to S. K. Mahata). The University of California, San Diego, School of Medicine Light Microscopy Facility is supported by the National Institute of Neurological Disorders and Stroke Grant NS047101.

DISCLOSURES

No conflicts of interest, financial or otherwise, are declared by the authors.

AUTHOR CONTRIBUTIONS

L.N., S.K.M., P.A.J., and E.C.B. conceived and designed research; L.N., A.E.Z.-H., R.Y., M.R., C.S., K.T., and E.C.B. performed experiments; L.N., A.E.Z.-H., R.Y., M.R., C.S., K.T., S.K.M., P.A.J., and E.C.B. analyzed data; L.N., A.E.Z.-H., R.Y., M.R., C.S., K.T., S.K.M., P.A.J., and E.C.B. interpreted results of experiments; L.N., A.E.Z.-H., S.K.M., and E.C.B. prepared figures; L.N., A.E.Z.-H., C.S., S.K.M., P.A.J., and E.C.B. drafted manuscript; L.N., A.E.Z.-H., R.Y., M.R., C.S., K.T., S.K.M., P.A.J., and E.C.B. edited and revised manuscript; L.N., A.E.Z.-H., R.Y., M.R., C.S., K.T., S.K.M., P.A.J., and E.C.B. approved final version of manuscript.

REFERENCES

1. **Vallone DM**, **Cuccia AF**, **Briggs J**, **Xiao H**, **Schillo BA**, **Hair EC.** Electronic cigarette and JUUL use among adolescents and young adults. *JAMA Pediatr* 174: 277–286, 2020 [Erratum in *JAMA Pediatr* 174: 305, 2020]. doi:10.1001/jamapediatrics.2019.5436.
2. **Jones K**, **Salzman GA.** The vaping epidemic in adolescents. *Mo Med* 117: 56–58, 2020.
3. **Perrine CG**, **Pickens CM**, **Boehmer TK**, **King BA**, **Jones CM**, **DeSisto CL**, **Duca LM**, **Lekiachvili A**, **Kenemer B**, **Shamout M**, **Landen MG**, **Lynfield R**, **Ghinai I**, **Heinzerling A**, **Lewis N**, **Pray IW**, **Tanz LJ**, **Patel A**, **Briss PA**, **Lung Injury Response Epidemiology/Surveillance Group.** Characteristics of a multistate outbreak of lung injury associated with e-cigarette use, or vaping—United States, 2019. *MMWR Morb Mortal Wkly Rep* 68: 860–864, 2019 [Erratum in *MMWR Morb Mortal Wkly Rep* 68: 900, 2019]. doi:10.15585/mmwr.mm6839e1.
4. **Miller C**, **Smith DM**, **Goniewicz ML.** Physical activity among adolescent tobacco and electronic cigarette users: cross-sectional findings from the Population Assessment of Tobacco and Health study. *Prev Med Rep* 15: 100897, 2019. doi:10.1016/j.pmedr.2019.100897.
5. **Merecz-Sadowska A**, **Sitarek P**, **Zielinska-Blizniewska H**, **Malinowska K**, **Zajdel K**, **Zakonnik L**, **Zajdel R.** A summary of in vitro and in vivo studies evaluating the impact of e-cigarette exposure on living organisms and the environment. *Int J Mol Sci* 21: 652, 2020. doi:10.3390/ijms21020652.
6. **Chatterjee S**, **Tao JQ**, **Johncola A**, **Guo W**, **Caporale A**, **Langham MC**, **Wehrli FW.** Acute exposure to e-cigarettes causes inflammation and pulmonary endothelial oxidative stress in nonsmoking, healthy young subjects. *Am J Physiol Lung Cell Mol Physiol* 317: L155–L166, 2019. doi:10.1152/ajplung.00110.2019.
7. **Chaumont M**, **van de Borne P**, **Bernard A**, **Van Muylem A**, **Deprez G**, **Ullmo J**, **Starczewska E**, **Briki R**, **de Hemptinne Q**, **Zaher W**, **Debbas N.** Fourth generation e-cigarette vaping induces transient lung inflammation and gas exchange disturbances: results from two randomized clinical trials. *Am J Physiol Lung Cell Mol Physiol* 316: L705–L719, 2019. doi:10.1152/ajplung.00492.2018.
8. **Kuntic M**, **Oelze M**, **Steven S**, **Kroller-Schon S**, **Stamm P**, **Kalinovic S**, **Frenis K**, **Vujacic-Mirski K**, **Bayo Jimenez MT**, **Kvandova M**, **Filippou K**, **Al Zuabi A**, **Bruckl V**, **Hahad O**, **Daub S**, **Varveri F**, **Gori T**, **Huesmann R**, **Hoffmann T**, **Schmidt FP**, **Keaney JF**, **Daiber A**, **Munzel T.** Short-term e-cigarette vapour exposure causes vascular oxidative stress and dysfunction: evidence for a close connection to brain damage and a key role of the phagocytic NADPH oxidase (NOX-2). *Eur Heart J* 41: 2472–2483, 2020. doi:10.1093/eurheartj/ehz772.
9. **Glynos C**, **Bibli SI**, **Katsaounou P**, **Pavlidou A**, **Magkou C**, **Karavana V**, **Topouzis S**, **Kalomenidis I**, **Zakynthinos S**, **Papapetropoulos A.** Comparison of the effects of e-cigarette vapor with cigarette smoke on lung function and inflammation in mice. *Am J Physiol Lung Cell Mol Physiol* 315: L662–L672, 2018. doi:10.1152/ajplung.00389.2017.
10. **Higham A**, **Bostock D**, **Booth G**, **Dungwa JV**, **Singh D.** The effect of electronic cigarette and tobacco smoke exposure on COPD bronchial epithelial cell inflammatory responses. *Int J Chron Obstruct Pulmon Dis* 13: 989–1000, 2018. doi:10.2147/COPD.S157728.
11. **Crotty Alexander LE**, **Drummond CA**, **Hepokoski M**, **Mathew D**, **Moshensky A**, **Willeford A**, **Das S**, **Singh P**, **Yong Z**, **Lee JH**, **Vega K**, **Du A**, **Shin J**, **Javier C**, **Tian J**, **Brown JH**, **Breen EC.** Translational physiology: chronic inhalation of e-cigarette vapor containing nicotine disrupts airway barrier function and induces systemic inflammation

and multiorgan fibrosis in mice. *Am J Physiol Regul Integr Comp Physiol* 314: R834–R847, 2018. doi:10.1152/ajpregu.00270.2017.

12. **Scott A**, **Lugg ST**, **Aldridge K**, **Lewis KE**, **Bowden A**, **Mahida RY**, **Grudzinska FS**, **Dosanjh D**, **Parekh D**, **Foronjy R**, **Sapey E**, **Naidu B**, **Thickett DR.** Pro-inflammatory effects of e-cigarette vapour condensate on human alveolar macrophages. *Thorax* 73: 1161–1169, 2018. doi:10.1136/thoraxjnl-2018-211663.
13. **Higham A**, **Rattray NJ**, **Dewhurst JA**, **Trivedi DK**, **Fowler SJ**, **Goodacre R**, **Singh D.** Electronic cigarette exposure triggers neutrophil inflammatory responses. *Respir Res* 17: 56, 2016. doi:10.1186/s12931-016-0368-x.
14. **Hwang JH**, **Lyes M**, **Sladewski K**, **Enany S**, **McEachern E**, **Mathew DP**, **Das S**, **Moshensky A**, **Bapat S**, **Pride DT**, **Ongkeko WM**, **Crotty Alexander LE.** Electronic cigarette inhalation alters innate immunity and airway cytokines while increasing the virulence of colonizing bacteria. *J Mol Med (Berl)* 94: 667–679, 2016. doi:10.1007/s00109-016-1378-3.
15. **Schweitzer KS**, **Chen SX**, **Law S**, **Van Demark M**, **Poirier C**, **Justice MJ**, **Hubbard WC**, **Kim ES**, **Lai X**, **Wang M**, **Kranz WD**, **Carroll CJ**, **Ray BD**, **Bittman R**, **Goodpaster J**, **Petrache I.** Endothelial disruptive proinflammatory effects of nicotine and e-cigarette vapor exposures. *Am J Physiol Lung Cell Mol Physiol* 309: L175–L187, 2015. doi:10.1152/ajplung.00411.2014.
16. **Sussan TE**, **Gajghate S**, **Thimmulappa RK**, **Ma J**, **Kim JH**, **Sudini K**, **Consolini N**, **Cormier SA**, **Lomnicki S**, **Hasan F**, **Pekosz A**, **Biswal S.** Exposure to electronic cigarettes impairs pulmonary anti-bacterial and anti-viral defenses in a mouse model. *PLoS One* 10: e0116861, 2015. doi:10.1371/journal.pone.0116861.
17. **Moheimani RS**, **Bhetraratana M**, **Peters KM**, **Yang BK**, **Yin F**, **Gornbein J**, **Araujo JA**, **Middlekauff HR.** Sympathomimetic effects of acute e-cigarette use: role of nicotine and non-nicotine constituents. *J Am Heart Assoc* 6: e006579, 2017. doi:10.1161/JAHA.117.006579.
18. **Chaumont M**, **de Becker B**, **Zaher W**, **Culié A**, **Deprez G**, **Mélot C**, **Reyé F**, **Van Antwerpen P**, **Delporte C**, **Debbas N**, **Boudjeltia KZ**, **van de Borne P.** Differential effects of e-cigarette on microvascular endothelial function, arterial stiffness and oxidative stress: a randomized crossover trial. *Sci Rep* 8: 10378, 2018. doi:10.1038/s41598-018-28723-0.
19. **Moheimani RS**, **Bhetraratana M**, **Yin F**, **Peters KM**, **Gornbein J**, **Araujo JA**, **Middlekauff HR.** Increased cardiac sympathetic activity and oxidative stress in habitual electronic cigarette users: implications for cardiovascular risk. *JAMA Cardiol* 2: 278–284, 2017. doi:10.1001/jamacardio.2016.5303.
20. **Buchanan ND**, **Grimmer JA**, **Tanwar V**, **Schwieterman N**, **Mohler PJ**, **Wold LE.** Cardiovascular risk of electronic cigarettes: a review of preclinical and clinical studies. *Cardiovasc Res* 116: 40–50, 2020. doi:10.1093/cvr/cvz256.
21. **Lee HW**, **Park SH**, **Weng MW**, **Wang HT**, **Huang WC**, **Lepor H**, **Wu XR**, **Chen LC**, **Tang MS.** E-cigarette smoke damages DNA and reduces repair activity in mouse lung, heart, and bladder as well as in human lung and bladder cells. *Proc Natl Acad Sci USA* 115: E1560–E1569, 2018. doi:10.1073/pnas.1718185115.
22. **Crotty Alexander LE**, **Drummond CA**, **Hepokoski M**, **Mathew D**, **Moshensky A**, **Willeford A**, **Das S**, **Singh P**, **Yong Z**, **Lee JH**, **Vega K**, **Du A**, **Shin J**, **Javier C**, **Tian J**, **Brown JH**, **Breen EC.** Chronic inhalation of e-cigarette vapor containing nicotine disrupts airway barrier function and induces systemic inflammation and multiorgan fibrosis in mice. *Am J Physiol Regul Integr Comp Physiol* 314: R834–R847, 2018 [Erratum in *Am J Physiol Regul Integr Comp Physiol* 323: R483, 2022]. doi:10.1152/ajpregu.00270.2017.
23. **Du A**, **Shin J**, **Lee JH**, **Breen EC**, **Vitorino SA**, **Crotty Alexander LE.** Heart rate and blood pressure effects of daily inhalation of nicotine containing e-cigarette vapor. *Am J Respir Crit Care Med* 195: A2045, 2017.
24. **Olfert IM**, **DeVallance E**, **Hoskinson H**, **Branyan KW**, **Clayton S**, **Pitzer CR**, **Sullivan DP**, **Breit MJ**, **Wu Z**, **Klinkhachorn P**, **Mandler WK**, **Erdreich BH**, **Ducatman BS**, **Bryner RW**, **Dasgupta P**, **Chantler PD.** Chronic exposure to electronic cigarettes results in impaired cardiovascular function in mice. *J Appl Physiol (1985)* 124: 573–582, 2018. doi:10.1152/japplphysiol.00713.2017.
25. **Chen YM**, **Huang CC**, **Sung HC**, **Lee MC**, **Hsiao CY.** Electronic cigarette exposure reduces exercise performance and changes the biochemical profile of female mice. *Biosci Biotechnol Biochem* 83: 2318–2326, 2019. doi:10.1080/09168451.2019.1651627.
26. **Fell RD**, **Terblanche SE**, **Winder WW**, **Holloszy JO.** Adaptive responses of rats to prolonged treatment with epinephrine. *Am J Physiol Cell Physiol* 241: C55–C58, 1981. doi:10.1152/ajpcell.1981.241.1.C55.
27. **Vu CU**, **Siddiqui JA**, **Wadensweiler P**, **Gayen JR**, **Avolio E**, **Bandyopadhyay GK**, **Biswas N**, **Chi N-W**, **O'Connor DT**, **Mahata SK.** Nicotinic acetylcholine receptors in glucose homeostasis: the acute hyperglycemic and chronic insulin-sensitive effects of nicotine suggest dual opposing roles of the receptors in male mice. *Endocrinology* 155: 3793–3805, 2014. doi:10.1210/en.2014-1320.
28. **Larsson L**, **Orlander J**, **Ansved T**, **Edström L.** Effects of chronic nicotine exposure on contractile enzyme-histochemical and biochemical properties of fast- and slow-twitch skeletal muscles in the rat. *Acta Physiol Scand* 134: 519–527, 1988. doi:10.1111/j.1748-1716.1998.tb08526.x.
29. **Young DA**, **Wallberg-Henriksson H**, **Cranshaw J**, **Chen M**, **Holloszy JO.** Effect of catecholamines on glucose uptake and glycogenolysis in rat skeletal muscle. *Am J Physiol Cell Physiol* 248: C406–C409, 1985. doi:10.1152/ajpcell.1985.248.5.C406.
30. **Juhlin-Dannfelt AC**, **Terblanche SE**, **Fell RD**, **Young JC**, **Holloszy JO.** Effects of beta-adrenergic receptor blockade on glycogenolysis during exercise. *J Appl Physiol Respir Environ Exerc Physiol* 53: 549–554, 1982. doi:10.1152/jappl.1982.53.3.549.
31. **Balezina OP**, **Fedorin VV**, **Gaidukov AE.** Effect of nicotine on neuromuscular transmission in mouse motor synapses. *Bull Exp Biol Med* 142: 17–21, 2006. doi:10.1007/s10517-006-0280-3.
32. **Chibalin AV**, **Heiny JA**, **Benziane B**, **Prokofiev AV**, **Vasiliev AV**, **Kravtsova VV**, **Krivoi II.** Chronic nicotine modifies skeletal muscle Na,K-ATPase activity through its interaction with the nicotinic acetylcholine receptor and phospholemman. *PLoS One* 7: e33719, 2012. doi:10.1371/journal.pone.0033719.
33. **Tang K**, **Wagner PD**, **Breen EC.** TNF-alpha-mediated reduction in PGC-1α may impair skeletal muscle function after cigarette smoke exposure. *J Cell Physiol* 222: 320–327, 2010. doi:10.1002/jcp.21955.
34. **Nogueira L**, **Trisko BM**, **Lima-Rosa FL**, **Jackson J**, **Lund-Palau H**, **Yamaguchi M**, **Breen EC.** Cigarette smoke directly impairs skeletal muscle function through capillary regression and altered myofibre calcium kinetics in mice. *J Physiol* 596: 2901–2916, 2018. doi:10.1113/JP275888.
35. **Maltais F**, **Decramer M**, **Casaburi R**, **Barreiro E**, **Burelle Y**, **Debigaré R**, **Dekhuijzen PN**, **Franssen F**, **Gayan-Ramirez G**, **Gea J**, **Gosker HR**, **Gosselink R**, **Hayot M**, **Hussain SN**, **Janssens W**, **Polkey MI**, **Roca J**, **Saey D**, **Schols AM**, **Spruit MA**, **Steiner M**, **Taivassalo T**, **Troosters T**, **Vogiatzis I**, **Wagner PD**; **ATS/ERS Ad Hoc Committee on Limb Muscle Dysfunction in COPD.** An official American Thoracic Society/European Respiratory Society statement: update on limb muscle dysfunction in chronic obstructive pulmonary disease. *Am J Respir Crit Care Med* 189: e15–e62, 2014. doi:10.1164/rccm.201402-0373ST.
36. **Kapchinsky S**, **Vuda M**, **Miguez K**, **Elkrief D**, **de Souza AR**, **Baglole CJ**, **Aare S**, **MacMillan NJ**, **Baril J**, **Rozakis P**, **Sonjak V**, **Pion C**, **Aubertin-Leheudre M**, **Morais JA**, **Jagoe RT**, **Bourbeau J**, **Taivassalo T**, **Hepple RT.** Smoke-induced neuromuscular junction degeneration precedes the fibre type shift and atrophy in chronic obstructive pulmonary disease. *J Physiol* 596: 2865–2881, 2018. doi:10.1113/JP275558.
37. **National Academies of Sciences EaM, Health and Medicine D, Board on Population Health and Public Health Practice, and Committee on the Review of the Health Effects of Electronic Nicotine Delivery Systems**. E-Cigarette Devices, Uses, and Exposures. In: *Public Health Consequences of E-Cigarettes*, edited by Eaton DL, Kwan LY, Stratton K. Washington, DC: National Academies Press, 2018.
38. **Ruschhaupt DG**, **Sodt PC**, **Hutcheon NA**, **Arcilla RA.** Estimation of circumferential fiber shortening velocity by echocardiography. *J Am Coll Cardiol* 2: 77–84, 1983. doi:10.1016/s0735-1097(83)80379-9.
39. **Zemljic-Harpf AE**, **Miller JC**, **Henderson SA**, **Wright AT**, **Manso AM**, **Elsherif L**, **Dalton ND**, **Thor AK**, **Perkins GA**, **McCulloch AD**, **Ross RS.** Cardiac-myocyte-specific excision of the vinculin gene disrupts cellular junctions, causing sudden death or dilated cardiomyopathy. *Mol Cell Biol* 27: 7522–7537, 2007. doi:10.1128/MCB.00728-07.
40. **Okada K**, **Mikami T**, **Kaga S**, **Onozuka H**, **Inoue M**, **Yokoyama S**, **Nishino H**, **Nishida M**, **Matsuno K**, **Iwano H**, **Yamada S**, **Tsutsui H.** Early diastolic mitral annular velocity at the interventricular septal

annulus correctly reflects left ventricular longitudinal myocardial relaxation. *Eur J Echocardiogr* 12: 917–923, 2011. doi:10.1093/ejechocard/jer154.

41. **Zemljic-Harpf AE**, **See Hoe LE**, **Schilling JM**, **Zuniga-Hertz JP**, **Nguyen A**, **Vaishnav YJ**, **Belza GJ**, **Budiono BP**, **Patel PM**, **Head BP**, **Dillmann WH**, **Mahata SK**, **Peart JN**, **Roth DM**, **Headrick JP**, **Patel HH.** Morphine induces physiological, structural, and molecular benefits in the diabetic myocardium. *FASEB J* 35: e21407, 2021. doi:10.1096/fj.201903233R.
42. **Ying W**, **Tang K**, **Avolio E**, **Schilling JM**, **Pasqua T**, **Liu MA**, **Cheng H**, **Gao H**, **Zhang J**, **Mahata S**, **Ko MS**, **Bandyopadhyay G**, **Das S**, **Roth DM**, **Sahoo D**, **Webster NJG**, **Sheikh F**, **Ghosh G**, **Patel HH**, **Ghosh P**, **van den Bogaart G**, **Mahata SK.** Immunosuppression of macrophages underlies the cardioprotective effects of CST (catestatin). *Hypertension* 77: 1670–1682, 2021. doi:10.1161/HYPERTENSIONAHA.120.16809.
43. **Carroll NV**, **Longley RW**, **Roe JH.** The determination of glycogen in liver and muscle by use of anthrone reagent. *J Biol Chem* 220: 583–593, 1956.
44. **Zuo L**, **Nogueira L**, **Hogan MC.** Effect of pulmonary TNF-alpha overexpression on mouse isolated skeletal muscle function. *Am J Physiol Regul Integr Comp Physiol* 301: R1025–R1031, 2011. doi:10.1152/ajpregu.00126.2011.
45. **Mahata SK**, **Mahapatra NR**, **Mahata M**, **Wang TC**, **Kennedy BP**, **Ziegler MG**, **O'Connor DT.** Catecholamine secretory vesicle stimulus-transcription coupling in vivo. Demonstration by a novel transgenic promoter/photoprotein reporter and inhibition of secretion and transcription by the chromogranin A fragment catestatin. *J Biol Chem* 278: 32058–32067, 2003. doi:10.1074/jbc.M305545200.
46. **Jall S**, **De Angelis M**, **Lundsgaard AM**, **Fritzen AM**, **Nicolaisen TS**, **Klein AB**, **Novikoff A**, **Sachs S**, **Richter EA**, **Kiens B**, **Schramm KW**, **Tschöp MH**, **Stemmer K**, **Clemmensen C**, **Müller TD**, **Kleinert M.** Pharmacological targeting of α3β4 nicotinic receptors improves peripheral insulin sensitivity in mice with diet-induced obesity. *Diabetologia* 63: 1236–1247, 2020. doi:10.1007/s00125-020-05117-4.
47. **Mahata SK**, **O'Connor DT**, **Mahata M**, **Yoo SH**, **Taupenot L**, **Wu H**, **Gill BM**, **Parmer RJ.** Novel autocrine feedback control of catecholamine release. A discrete chromogranin a fragment is a noncompetitive nicotinic cholinergic antagonist. *J Clin Invest* 100: 1623–1633, 1997. doi:10.1172/JCI119686.
48. **Real-Martinez A**, **Brull A**, **Huerta J**, **Tarrasó G**, **Lucia A**, **Martin MA**, **Arenas J**, **Andreu AL**, **Nogales-Gadea G**, **Vissing J**, **Krag TO**, **de Luna N**, **Pinós T.** Low survival rate and muscle fiber-dependent aging effects in the McArdle disease mouse model. *Sci Rep* 9: 5116, 2019. doi:10.1038/s41598-019-41414-8.
49. **Ingalls CP**, **Wenke JC**, **Nofal T**, **Armstrong RB.** Adaptation to lengthening contraction-induced injury in mouse muscle. *J Appl Physiol (1985)* 97: 1067–1076, 2004. doi:10.1152/japplphysiol.01058.2003.
50. **Brown GL**, **Bülbring E**, **Burns BD.** The action of adrenaline on mammalian skeletal muscle. *J Physiol* 107: 115–128, 1948. doi:10.1113/jphysiol.1948.sp004255.
51. **Cairns SP**, **Dulhunty AF.** The effects of beta-adrenoceptor activation on contraction in isolated fast- and slow-twitch skeletal muscle fibres of the rat. *Br J Pharmacol* 110: 1133–1141, 1993. doi:10.1111/j.1476-5381.1993.tb13932.x.
52. **Andersson DC**, **Betzenhauser MJ**, **Reiken S**, **Umanskaya A**, **Shiomi T**, **Marks AR.** Stress-induced increase in skeletal muscle force requires protein kinase A phosphorylation of the ryanodine receptor. *J Physiol* 590: 6381–6387, 2012. doi:10.1113/jphysiol.2012.237925.
53. **Felmus MT**, **Patten BM**, **Hart A**, **Martinez C.** Catecholamine-induced muscle weakness. *Arch Neurol* 34: 280–284, 1977. doi:10.1001/archneur.1977.00500170034005.
54. **Krnjevic K**, **Miledi R.** Adrenaline and failure of neuromuscular transmission. *Nature* 180: 814–815, 1957. doi:10.1038/180814b0.
55. **Cryer PE.** Disorders of sympathetic neural function in human diabetes mellitus: hypoadrenergic and hyperadrenergic postural hypotension. *Metabolism* 29: 1186–1189, 1980. doi:10.1016/0026-0495(80)90028-1.
56. **Wolfe RR**, **Shaw JH.** Effect of epinephrine infusion and adrenergic blockade on glucose oxidation in conscious dogs. *Metabolism* 35: 673–678, 1986. doi:10.1016/0026-0495(86)90177-0.
57. **Träger K**, **Radermacher P.** Catecholamines in the treatment of septic shock: effects beyond perfusion. *Crit Care Resusc* 5: 270–276, 2003.
58. **Träger K**, **Radermacher P**, **Debacker D**, **Vogt J**, **Jakob S**, **Ensinger H.** Metabolic effects of vasoactive agents. *Curr Opin Anaesthesiol* 14: 157–163, 2001. doi:10.1097/00001503-200104000-00006.
59. **MacGregor DA**, **Prielipp RC**, **Butterworth JF**, **James RL**, **Royster RL.** Relative efficacy and potency of β-adrenoceptor agonists for generating cAMP in human lymphocytes. *Chest* 109: 194–200, 1996. doi:10.1378/chest.109.1.194.
60. **Macdonald IA**, **Bennett T**, **Fellows IW.** Catecholamines and the control of metabolism in man. *Clin Sci (Lond)* 68: 613–619, 1985. doi:10.1042/cs0680613.
61. **Raz I**, **Katz A**, **Spencer MK.** Epinephrine inhibits insulin-mediated glycogenesis but enhances glycolysis in human skeletal muscle. *Am J Physiol Endocrinol Physiol* 260: E430–E435, 1991. doi:10.1152/ajpendo.1991.260.3.E430.
62. **Laurent D**, **Petersen KF**, **Russell RR**, **Cline GW**, **Shulman GI.** Effect of epinephrine on muscle glycogenolysis and insulin-stimulated muscle glycogen synthesis in humans. *Am J Physiol Endocrinol Physiol* 274: E130–E138, 1998. doi:10.1152/ajpendo.1998.274.1.E130.
63. **Bozier J**, **Chivers EK**, **Chapman DG**, **Larcombe AN**, **Bastian NA**, **Masso-Silva JA**, **Byun MK**, **McDonald CF**, **Crotty Alexander LE**, **Ween MP.** The evolving landscape of e-cigarettes: a systematic review of recent evidence. *Chest* 157: 1362–1390, 2020. doi:10.1016/j.chest.2019.12.042.
64. **Liu RH**, **Mizuta M**, **Matsukura S.** Long-term oral nicotine administration reduces insulin resistance in obese rats. *Eur J Pharmacol* 458: 227–234, 2003. doi:10.1016/s0014-2999(02)02726-7.
65. **Xu TY**, **Guo LL**, **Wang P**, **Song J**, **Le YY**, **Viollet B**, **Miao CY.** Chronic exposure to nicotine enhances insulin sensitivity through α7 nicotinic acetylcholine receptor-STAT3 pathway. *PLoS One* 7: e51217, 2012. doi:10.1371/journal.pone.0051217.
66. **Tsentsevitsky AN**, **Kovyazina IV**, **Bukharaeva EA.** Diverse effects of noradrenaline and adrenaline on the quantal secretion of acetylcholine at the mouse neuromuscular junction. *Neuroscience* 423: 162–171, 2019. doi:10.1016/j.neuroscience.2019.10.049.
67. **Zile MR**, **Brutsaert DL.** New concepts in diastolic dysfunction and diastolic heart failure: Part II: causal mechanisms and treatment. *Circulation* 105: 1503–1508, 2002. doi:10.1161/hc1202.105290.
68. **McCully KK**, **Faulkner JA.** Injury to skeletal muscle fibers of mice following lengthening contractions. *J Appl Physiol (1985)* 59: 119–126, 1985. doi:10.1152/jappl.1985.59.1.119.
69. **Heiny JA**, **Kravtsova VV**, **Mandel F**, **Radzyukevich TL**, **Benziane B**, **Prokofiev AV**, **Pedersen SE**, **Chibalin AV**, **Krivoi II.** The nicotinic acetylcholine receptor and the Na,K-ATPase alpha2 isoform interact to regulate membrane electrogenesis in skeletal muscle. *J Biol Chem* 285: 28614–28626, 2010. doi:10.1074/jbc.M110.150961.
70. **Lovering RM**, **Roche JA**, **Goodall MH**, **Clark BB**, **McMillan A.** An in vivo rodent model of contraction-induced injury and non-invasive monitoring of recovery. *J Vis Exp* 51: e2782, 2011. doi:10.3791/2782.